# Electron Multiplication Process in Proportional Counters*

RAYMOND GOLD AND EDGAR F. BENNETT
*Argonne National Laboratory, Argonne, Illinois*
(Received 10 January 1966)

The electron multiplication process in proportional counters has been investigated by observing the counter response to single electrons in a manner similar to the original experiment of Curran, Cockroft, and Angus. The single-electron pulse-height spectrum has been measured over a range of anode voltages for a number of different argon-methane counter gas mixtures. The behavior of the gas amplification as a function of anode voltage is used as a criterion to determine proper proportional counter operation. The single-electron pulse-height spectrum obtained in the present measurements is not constant but depends upon the average final number of electrons in the avalanche. This behavior is attributed to the fact that the electron branching process in proportional counters is non-Markovian. Two non-Markovian branching models are introduced and the asymptotic behavior of these models is compared with experimental results.

## I. INTRODUCTION

GAS-filled proportional counters have been utilized in many different areas of experimental nuclear physics for more than two decades. In view of the broad applicability of this counter, a complete understanding of the detection mechanism is important. We shall be concerned with only one aspect of this detection process, namely the electron multiplication or avalanche phenomenon which arises in such a gas-filled proportional counter. Actually this multiplication process can be defined in terms of single electrons that drift into the center wire of the counter. Only in this case, i.e., with single electrons, can one study the statistics of the multiplication process alone.

The response distribution due to single electrons was first measured by Curran, Cockroft, and Angus[1] who employed ultraviolet quanta to release single electrons (by means of the photoelectric effect) into the active counter volume. Utilizing a proportional counter filled with a 50% methane–50% argon mixture, Curran *et al.*, deduced the probability distribution, $P(n)$, for the final number of electrons from the multiplication process. That is, $P(n)dn$ represents the probability of the multiplication process resulting in a final number of electrons between $n$ and $n+dn$. Their experimental results could be described in a normalized form as

$$P(\nu)=\frac{2}{\sqrt{\pi}}\nu^{1/2}e^{-\nu}, \tag{1}$$

where

$$\nu=n/\bar{n}, \tag{2}$$

with $\bar{n}$ the average final number of electrons in the avalanche.

Using a proportional counter with the same gas mixture, a similar single-electron experiment was performed at Oak Ridge National Laboratory.[2] The probability distribution deduced from these observations was of the form

$$P(\nu)=e^{-\nu}. \tag{3}$$

Perhaps the most apparent difference between these two experiments, as reported, lies in the fact that the gas amplification was significantly different. For single-electron measurements, the gas amplification or gas gain is merely $\bar{n}$. The measurement of Curran *et al.*, corresponded to a value of $\bar{n}\cong 1.5\times 10^5$, whereas the experiment conducted at ORNL utilized $\bar{n}\cong 4\times 10^4$.

The exponential distribution given in Eq. (3) is in agreement with the theoretical work of Frisch[3,4] and Snyder,[5] who utilize a simple discrete Markovian branching process to describe the electron avalanche. More recently, Byrne[6] and Lansiart and Morucci[7] have independently proposed a model in which the first Townsend coefficient, $\alpha$, (i.e. the number of ion pairs created by an electron per unit path length) depends on the total number of electrons already produced in the avalanche. This assumption leads to a description of the avalanche as a nonstationary discrete Markovian branching process. For the same special form of $\alpha$, both Byrne and Lansiart and Morucci obtain the probability distribution given in Eq. (1), in agreement with the experimental observations of Curran *et al.*[1] However, it is not clear that this model is meaningful since it rests upon the experimental evidence of Curran *et al.*, which, in turn, has been subject to some dispute.[2]

In addition to clarifying the above issue, an improved definition of the multiplication process can provide a better understanding of low-energy ionization phenomena in gases. At low energy, the multiplication process can significantly broaden experimental measurements. Consequently, the low-energy limit of the applicability of proportional counters must rest, at least partially, upon a knowledge of this multiplication process. Moreover, any extension of the low-energy bound

* Work performed under the auspices of the U. S. Atomic Energy Commission.
[1] S. C. Curran, A. L. Cockroft, and J. Angus., Phil. Mag. **40**, 929 (1949).
[2] Oak Ridge National Laboratory, Health Physics Division Annual Progress Report, ORNL-2994, 1960 (unpublished), p. 210.
[3] O. R. Frisch, 1948 (unpublished lectures).
[4] O. R. Frisch, CRL-57 (AECL No. 748), 1959 (unpublished).
[5] H. S. Snyder, Phys. Rev. **72**, 181 (1947).
[6] J. Byrne, Proc. Roy. Soc. Edinburg, **A66**, 33 (1961–1962).
[7] A. Lansiart and J. P. Morucci, J. Phys. Radium **23**, Suppl. No. 6, 102A (1962).

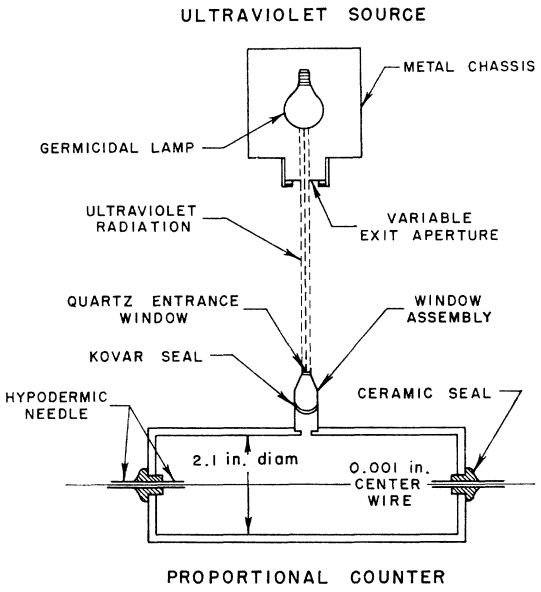


FIG. 1. Experimental arrangement of proportional counter, window assembly, and ultraviolet source.

of the usefulness of proportional counters must entail a more precise knowledge of the electron avalanche. This is true, for example, in the application of $4\pi$–hydrogen-recoil proportional counters utilized in the measurement of fast-neutron spectra.[8]

The experimental method used to measure single electron response distributions is described in detail below. In the following section, the experimental data obtained with this apparatus are presented and then these results are discussed. In the concluding section, the experimental evidence is utilized in an effort to provide a basic description of the electron branching process in proportional counters.

## II. EXPERIMENTAL METHOD

Figure 1 depicts the experimental arrangement which is not essentially different from the original experiment of Curran, Cockroft, and Angus.[1] A cylindrical proportional counter body of 2.25 in. diameter was constructed of 0.060-in. thick stainless steel. A 0.001-in. diameter stainless steel wire served as the anode. The anode wire was centered in the cathode by means of hypodermic needles which were, in turn, positioned in ceramic seals at each end of the counter body.

The window assembly soldered to the counter body, as shown in Fig. 1, provided an entrance slit for ultraviolet quanta. The window itself was made of quartz so as not to attenuate ultraviolet radiation. Ultraviolet quanta enter the counter window, traverse the active counter volume, and create photoelectrons at the opposite counter wall. A 4-W germicidal lamp (GE No. 58G827) served as the source of ultraviolet quanta. In order to provide more geometric definition for the source, the lamp was enclosed in a metal chassis which, in turn, was provided with a circular exit aperture. The ultraviolet intensity could be varied by either changing the diameter of the exit aperture or by moving the entire source assembly on a guided track. The proportional counter was fixed at one end of this track and surrounded by lead brick to provide shielding against external background. The background count rate was usually a few counts per second and the total count rate for measurements of the single electron spectra never exceeded a few thousand per second.

A low-noise preamplifier was mounted at one end of the body of the counter. Signals from the preamplifier were amplified and fed into two channels. One channel provided standard amplified pulses for subsequent pulse height analysis. In the second channel the amplified pulses fed an integral discriminator which generated an appropriate analyzer gate pulse.

Single electron distributions were investigated using different mixtures of argon and methane. The four counter fillings reported here are designated in Table I as counters I, II, III, and IV, respectively. Under these conditions, single electron spectra were observed over a range of anode voltage for each gas mixture. Anode voltages ranged between 2000 and 3700 V for the different mixtures utilized in these measurements.

A small amount of nitrogen, usually a partial pressure of a few cm of mercury, was added to each counter filling. Introduction of the nitrogen afforded use of the $N^{14}(n,p)C^{14}$ reaction as a convenient means of evaluating counter operation. The counter was placed in the center of a small moderating assembly which contained a plutonium-beryllium neutron source ($\sim 5\times 10^6$ n/sec). In this environment, monoenergetic protons from the exoergic $N^{14}(n,p)C^{14}$ reaction arise throughout the entire body of the counter.

Measurement of this monoenergetic event serves two important functions. First, it permits an examination of the resolution of the counter as a test for proper quality of operation. The resolution (i.e. relative full width at half-maximum) varied from about 5 to 7% for the different gas mixtures utilized. Figure 2 displays the response to this monoenergetic event in counter I with an anode voltage of 1000 V.

The second important function provided by the $N^{14}(n,p)C^{14}$ reaction is the calibration of the gas gain

TABLE I. Proportional counter gas mixtures.[a]

| | Partial Pressure | | |
|---|---|---|---|
| | Methane | Argon | Nitrogen |
| Counter I | 10 | 76 | 4 |
| Counter II | 20 | 76 | 4 |
| Counter III | 76 | 0 | 4 |
| Counter IV | 38 | 0 | 2 |

[a] The partial pressures are given in units of centimeters of mercury.

[8] E. F. Bennett, Argonne National Laboratory-6897, 1964 (unpublished).

of the proportional counter as a function of the anode voltage. The absolute gas amplification can be determined from a knowledge of the charge that is collected directly from the proportional counter corresponding to the pulse height of the monoenergetic $N^{14}(n,p)C^{14}$ event. Additional knowledge concerning the average number of electrons generated in the gas by this monoenergetic event is necessary. In order to estimate the average number of electrons, $\bar{N}_e$, so created, assumptions must be employed for the effective proton energy or effective $Q$ of the reaction as well as for the value of $W$ (the average energy loss per ion pair) for protons in the gas. Table II contains the parameters that have been utilized for counters I, II, III, and IV.

The experimental data of gas amplification so obtained has been treated according to the empirical formula introduced by Diethorn.[9] This formula, which relates gas amplification A and anode voltage V, follows from certain assumptions introduced in the conventional description of the multiplication process. In this picture, the initiating electron drifts, in approximate equilibrium with the gas to within a diameter or so of the anode wire. Here the electric field $E$ is strong enough to allow the electron to gain energy sufficient to ionize molecules of the gas. Secondary electrons so produced will contribute further to the process, and an avalanche with an increase in number of $10^5$ or more may result.

It is customary to introduce the quantity $\alpha$, defined as the mean number of secondary electrons produced by an electron per centimeter of path. The reciprocal of $\alpha$ is the mean free path for ionizing collisions. If $A$ is the number of electrons at the wire surface ($r=a$), then according to the definition of $\alpha$,

$$\ln A=\int_a^{r_c}\alpha(r)dr, \tag{4}$$

where $r_c$ is the critical distance at which the electron is first able to multiply. In principle, then, from knowledge of $\alpha$ and its dependence on electric field strength $E$, Eq. (4) can be integrated to give $A$ in terms of counter parameters. The principal difficulty is that data on $\alpha$ are not extensive, and the form that the results would take would not be convenient for quickly determining the effects of voltage changes for the many different gas mixtures used in proportional counters.

TABLE II. $N^{14}(n,p)C^{14}$ reaction constants.

| | $Q$,[a] keV | $W$, eV | $\bar{N}_e$ ($\times 10^4$) |
|---|---|---|---|
| Counter I | 615 | 26.4 | 2.33 |
| Counter II | 615 | 26.4 | 2.33 |
| Counter III | 615 | 29.4 | 2.09 |
| Counter IV | 615 | 29.4 | 2.09 |

[a] This value is not the true $Q$ of the reaction, but is the estimated equivalent proton energy which arises in gas.

[9] W. Diethorn, NYO-6628, 1956 (unpublished).

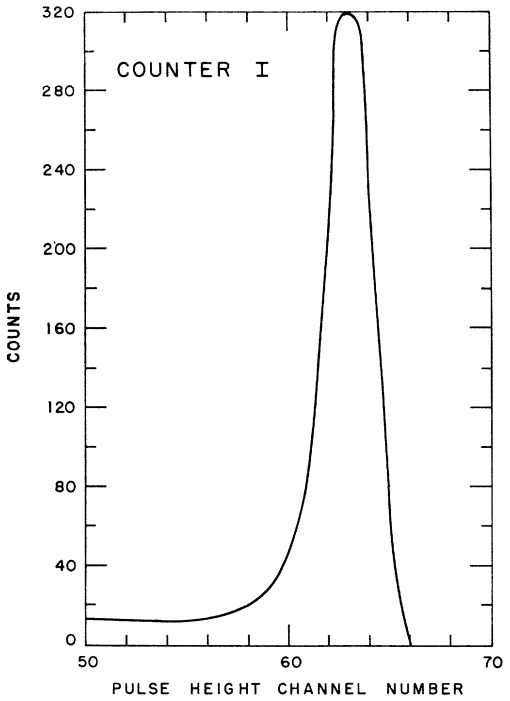


FIG. 2. Pulse-height response distribution from the $N^{14}(n,p)C^{14}$ reaction in counter I with an anode voltage of 1000 V (resolution $\cong$4.5%).

In a proportional counter, the electric field $E$ depends upon anode radius $a$, cathode radius $b$, anode voltage V, and distance $r$, as

$$E=\frac{V}{r\ln(b/a)}. \tag{5}$$

Consequently, one can write

$$\ln A=\int_{E(a)}^{E(r_c)}\alpha(E)\frac{\partial r}{\partial E}dE. \tag{6}$$

Introducing Eq. (5), one finds

$$\ln A=\frac{V}{\ln(b/a)}\int_{E(r_c)}^{E(a)}\frac{\alpha(E)}{E}\frac{dE}{E}. \tag{7}$$

To facilitate the use of proportional counters, various analytical approximations of $\alpha$ have been made. Rose and Korff[10] introduced an effective $\alpha$ with a $E^{1/2}$ field dependence whereas Diethorn[9] assumed that $\alpha$ should be directly proportional to the field strength $E$. The formulas that result from Eq. (7) for both these assumptions have been independently tested by many investigators.[11–13] These experimental measurements

[10] M. E. Rose and S. A. Korff, Phys. Rev. **59**, 850 (1941).
[11] R. W. Kiser, Appl. Sci. Res. B **8**, 183 (1960).
[12] A. Williams and R. I. Sara, J. Appl. Rad. Isotopes **13**, 229 (1962).
[13] G. E. Kocharov and G. A. Korolev, Bull. Acad. Sci. USSR, Phys. Ser. **27**, 308 (1963).

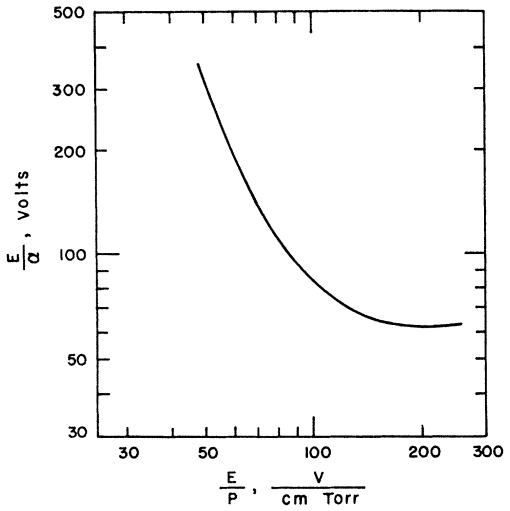


FIG. 3. The behavior of $E/\alpha$ as a function of $E/p$ for methane.

show that both results provide reliable descriptions of gas amplification in proportional counters.

Specht and Armbruster[14] have recently investigated proportional counter operation with a gas flow counter, and unusually high field-to-pressure ratios, $E/p>10^3$ $V$/cm Torr, where $p$ is the gas pressure. This work indicates that the Rose and Korff formula is superior to that of Diethorn in this region of operation. However, in the present investigation, measurements have been confined to the customary region of proportional counter operation, $E/p<10^3$ $V$/cm Torr. In this region, the general validity of Diethorn's formula can also be established on theoretical grounds.

Measurements of $(\alpha/E)$ as a function of $(E/p)$ demonstrate that $(\alpha/E)$ is a well-behaved function. For example, Fig. 3 displays $(E/\alpha)$ as a function of $(E/p)$ for methane after Schlumbohm.[15] Therefore, one can assume that $[\alpha(E)/E]$ is a continuous function and it follows that the law of the mean can be applied in Eq. (7). The result can be written in the form

$$\ln A=\frac{V}{\ln(b/a)}(\alpha/E)_i \ln\left[\frac{E(a)}{E(r_c)}\right]. \tag{8}$$

Here the notation $(\alpha/E)_i$, in Eq. (8), denotes the appropriate intermediate value for the function $[\alpha(E)/E]$ in the interval $[E(r_c),E(a)]$. Since the upper limit, $E(a)$, is a function of the anode voltage $V$, then $(\alpha/E)_i$ must also be a function of $V$. This fact is expressed by utilizing the notation $(\alpha/E)_i\equiv[(\alpha/E)(V)]_i$. Introducing $K$ as the critical field-to-pressure ratio at $r_c$, Eq. (8) takes the form

$$\frac{\ln A}{V}=\frac{[(\alpha/E)(V)]_i}{\ln(b/a)}\ln\left[\frac{V}{Kpa\ln(b/a)}\right]. \tag{9}$$

[14] H. J. Specht and P. Armbruster, Nukleonik **7**, 8 (1965).
[15] H. Schlumbohm, Z. Physik. **151**, 563 (1958).

The Diethorn representation of gas gain follows from Eq. (9) by assuming $[(\alpha/E)(V)]_i$ is a constant, independent of $V$.

It is clear from the origin of the term $[(\alpha/E)(V)]_i$, that it will be a slowly varying function of $V$. Moreover, for most gases $(\alpha/E)$, itself, becomes a slowly varying function of $(E/p)$, for large enough values of $(E/p)$. This behavior is clearly demonstrated for methane in Fig. 3. Since the usual domain of values of $K$, for gases of interest, occurs in this slowly varying region, then $[(\alpha/E)(V)]_i$ will be a very slowly varying function of $V$. Hence, it follows that Diethorn's formula should provide an adequate approximation for proportional counter operation in the region $E/p<10^3$ $V$/cm Torr.

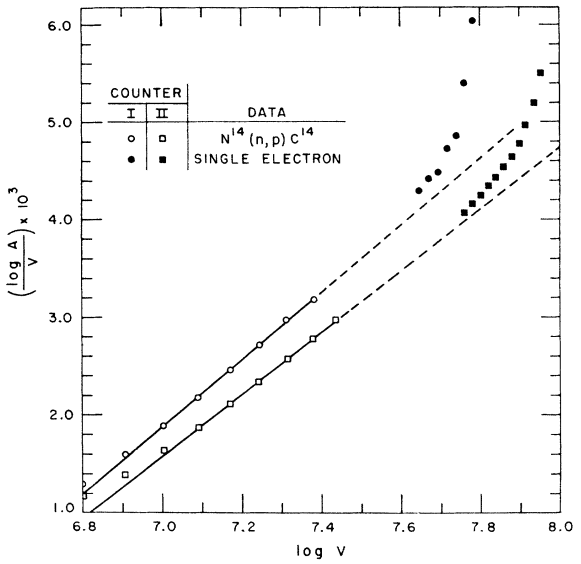


FIG. 4. The Diethron representation of gas amplification $A$ as a function of anode voltage $V$ for counters I and II.

This representation was extended to larger gas gains by employing the average $\bar{n}$ obtained from the single electron spectra at higher anode voltages. It should be noted that the large values of gas amplification obtained in this manner, do not depend upon the values introduced in Table II and utilized in the $N^{14}(n,p)C^{14}$ estimates of gas gain. Consequently, one must naturally expect that the complete Diethorn representation of gas amplification (which extends over six decades in the present observations) may be somewhat sensitive to the choice of these parameters.

This analysis plays a crucial role as a criterion for proper proportional counter operation in the region of very high gas amplification. Any serious deviation in the monotonically increasing behavior of gas amplification as a function of anode voltage must imply the onset of phenomena which have modified the normal electron multiplication process. In this manner one can restrict attention to only those single electron spectra which arise from the normal mode of operation of the propor-

tional counter. The utility of this criterion will be demonstrated by the experimental results obtained with counters I, II, III, and IV.

## III. EXPERIMENTAL RESULTS

The Diethorn representation of $A$ as a function of $V$, obtained for counters I and II, is displayed in Fig. 4. Note the rapid departure of the experimental data from the theoretical extrapolations at higher values of gas amplification. Actually counter II does not exhibit as drastic a departure from the theoretical extrapolation as does counter I. This behavior can be attributed to the fact that counter II contains twice the partial pressure of methane (20 cm of mercury) that counter I possesses (10 cm of mercury). It is well known that methane provides quenching of ultraviolet instabilities, which would otherwise influence the multiplication process.[10] While the quenching provided by 10 or 20 cm of methane may be adequate at customary values of gas gain, it is evident that this is not the case for the higher values of $A$ which occur in the measurement of single electron spectra.

Further verification of this deviation from proper proportional counter operation was obtained directly from the single electron spectra. At sufficiently high values of the anode voltage, complete discharge was observed for both counters I and II. For example, Fig. 5 depicts $P(\nu)$ as a function of $\nu$ for counter II at $V=2850$ V. The peak at the upper end of this spectrum corresponds to operation of this counter in a complete discharge mode. The gas gain corresponding to this mode of operation was approximately $1.3\times10^7$. (The corresponding gas gain for the discharge mode of counter I was approximately $1.7\times10^7$.) This conclusion was reaffirmed by examination of the counter response to radiation other than the single-electron type. Employing external gamma-ray sources, no response could be observed which exceeded the response level of this peak. Consequently, the single electron spectra obtained with counters I and II are almost exclusively confined to a "discharge-threshold" region. In this region, the contribution of ultraviolet photons to the multiplication process can no longer be considered negligible.

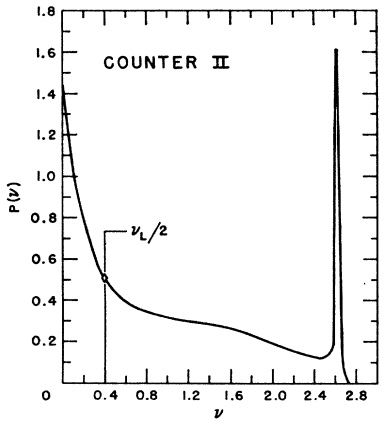


FIG. 5. Observation of the complete discharge mode of counter operation in the single-electron spectrum of counter II with $V=2850$ V.

Before introducing any further data, it is important to stress that the results already displayed in Fig. 4 and 5 above are dependent on the treatment of the experimental data. In the measurement of single electron spectra or, in fact, any other continuous spectra, distributions can only be observed over a finite range of pulse-height corresponding to the interval $\nu_L\leq\nu\leq\nu_U$. Here the lower bound $\nu_L$ represents the noise level of the preamplifier and amplifier system which masks the low pulse height end of the spectrum. The upper bound $\nu_U$ arises due to the limitation of finite preamplifier and amplifier gain. In order to obtain a complete picture of the spectrum ($0\leq\nu<\infty$), one must extrapolate the data obtained in the experimental "window" between these two bounds ($\nu_L\leq\nu\leq\nu_U$). Consequently the presentation of the data must depend on the extrapolations introduced in the regions $\nu\leq\nu_L$ and $\nu\geq\nu_U$.

In the region $\nu\geq\nu_U$, it has been assumed that the single electron spectrum behaves strictly as a decreasing exponential function. That this assumption is reasonable follows from an examination of the measurements of these single electron spectra. A semilog plot of the "tail" of these distributions reveals a linear dependence which justifies this assumption. The proper slope and normalization has been obtained from a linear least-squares fit of the logarithm of the data in the highest 20 to 35 pulse-height channels. The results obtained were almost independent of the number of points utilized in this least-squares fit. The variation which did arise, from a change in the number of channels so utilized, never exceeded a few percent. The demonstrated insensitivity of the results to the number of least-square points utilized furnishes additional justification for the extrapolation method introduced in the region $\nu\geq\nu_U$.

Unfortunately this insensitivity does not carry over to the extrapolation technique employed in the region $\nu\leq\nu_L$. In order to extend the data into channels normally occupied by noise level, the single electron distribution obtained at a given anode voltage was taken at two different values of amplifier gain. Since these two gain

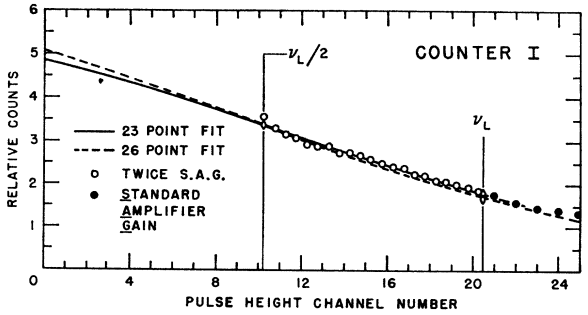


FIG. 6. Least-squares extrapolation of the experimental data in the region $\nu\leq(\nu_L/2)$ for counter I with an anode voltage of 2300 V.

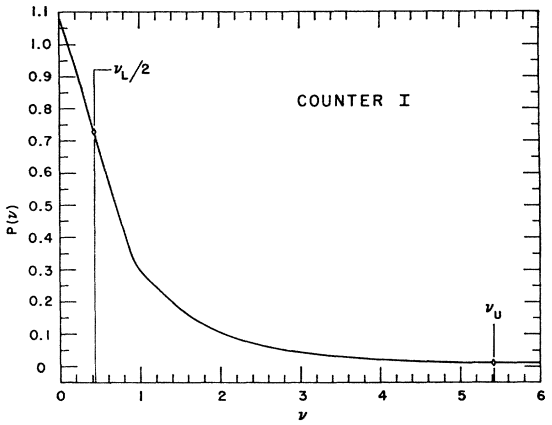


FIG. 7. The single-electron spectrum $P(\nu)$ versus $\nu$ for counter I with an anode voltage of 2300 V.

settings normally differed by a factor of two, the effective lower bound could be extended down to a channel corresponding to $(\nu_L/2)$. After proper normalization of this data, a single spectrum was obtained for the region $(\nu_L/2) \leq \nu \leq \nu_U$.

For the extrapolation in the region corresponding to $\nu \leq (\nu_L/2)$, a least-squares fit of the logarithm of the experimental data was also utilized. In this region, however, a second-degree fit was employed in an effort to follow the obvious curvature in the data at lower channels. The number of points utilized for this least-squares fit varied between ten and thirty. Figure 6 presents an example of this treatment of the data for counter I with an anode voltage of 2300 V. The least-squares fit obtained with both 23 and 26 points is presented. As discussed above, the data depicted in the interval $(\nu_L/2) \leq \nu \leq \nu_L$ in Fig. 6 were obtained at twice the amplifier gain utilized for the spectrum measurements in the region $\nu \geq \nu_L$.

There are many reasons for the increased sensitivity of this least-squares extrapolation in the region $\nu \leq (\nu_L/2)$ upon the number of points utilized. The very structure of these single electron spectra, which exhibit considerably more curvature in the lower pulse height channels, leads to considerable complications. In addition, any extrapolation that is introduced relies upon the tacit assumption that the single electron spectrum behaves smoothly below the lower bound. However, if too many channels are utilized in the least-squares technique, the extrapolation which results may be too heavily weighted by the data in the higher pulse-height channels. On the other hand, one must utilize enough points to provide a reasonably accurate least-squares fit and avoid uncertainties which could otherwise arise from counting statistics. Finally, the general monotonic decreasing behavior of single electron spectra with the increase to higher values of pulse height implies that errors which arise from our treatment of the data in the region $\nu \leq (\nu_L/2)$ are by far more heavily weighted than those which occur in the region $\nu \geq \nu_U$.

To illustrate this treatment of the data, Fig. 7 presents the distribution obtained for counter I with an anode voltage of 2300 V. The least-squares fit utilized here has already been displayed in Fig. 6. Since the distributions which arise from the 23- and 26-point extrapolations virtually coincide, only one curve for $P(\nu)$ is presented in Fig. 7. The upper and lower bounds $(\nu_L/2)$ and $\nu_U$ for this measurement are shown in Fig. 7. In the regions $\nu < (\nu_L/2)$ and $\nu > \nu_U$, the continuation of the experimental data is based on the extrapolation procedures discussed above.

In terms of the above discussion, it is evident that some criterion must be introduced which defines the proper measurement of a single-electron spectrum. Certainly for lower values of gas gain, only the "tail" of the single electron distribution will be observed above the noise level of the detection system. It is obvious that the spectrum of interest is not properly defined by such a measurement. Indeed, for such a case the major portion of the spectrum has actually not been observed. Furthermore, the moments of the spectrum which depend upon the methods of extrapolation that have been introduced, become much too sensitive to this treatment of the data to provide reliable or meaningful physical parameters which, in turn, describe the desired distribution.

Obviously the smaller the value of $(\nu_L/2)$ attained in any measurement, the greater the reliability one can give to not only the resulting distribution, but any further interpretations, such as moments, which are based upon the distribution. We shall impose the requirement $\nu_L < \bar{\nu} = 1$ (or equivalently $\nu_L/2 \leq 0.5$) as a necessary condition for the proper definition of a given single-electron spectrum. It is apparent that this condition does not define a sharp or abrupt boundary between well-defined and poorly defined spectra. This fact should be recognized and taken into account in assessing the data which are presented. For example, in the single electron spectra shown in Figs. 5 and 7, one finds $(\nu_L/2) \cong 0.4$. While the condition $(\nu_L/2) < 0.5$ is obviously satisfied for these spectra, it is also apparent from these figures that the spectral contribution below $(\nu_L/2)$ is not completely negligible. Consequently, one must regard this condition as only a rough index of the validity of a given single-electron spectrum measurement.

The data obtained with counters I and II point out that greater partial pressures of methane are necessary for quenching ultraviolet instabilities. These instabilities do not allow proper operation of the counter in the proportional region[16] and therefore the multiplication process which arises under these conditions cannot be attributed to a proportional counter.

Single-electron spectra have been observed in counter III. This counter may be regarded as a "pure" methane counter, except, of course, for the small addition of nitrogen. The gas amplification as a function of anode

[16] B. B. Rossi and H. H. Staub, *Ionization Chambers and Counters* (McGraw-Hill Book Company, Inc., New York, 1949).

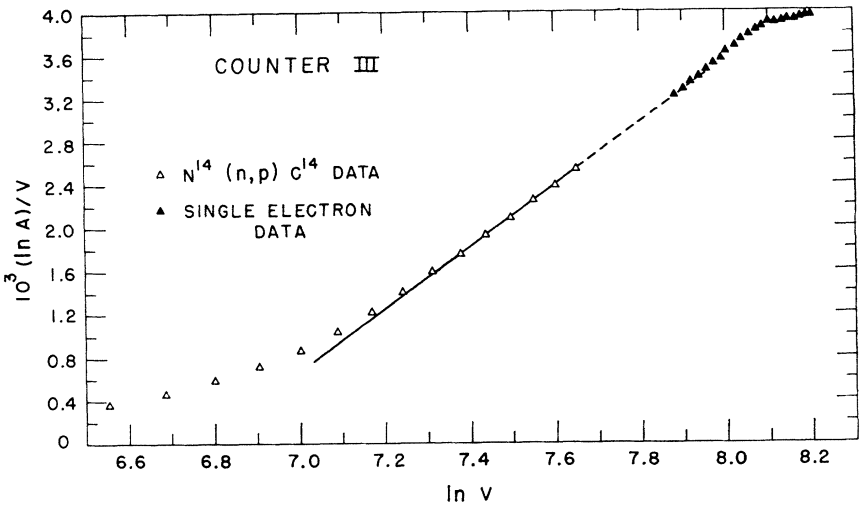


FIG. 8. The Diethorn representation of gas amplification $A$ as a function of anode voltage $V$ for counter III.

voltage obtained from counter III has also been treated according to Diethorn's formula. The results, which extend over a region of six decades in gas amplification, are presented in Fig. 8. Examination of these results reveals that, in general, the gas gain $A$ increases at a slightly higher rate than that which is predicted.

In contrast to the behavior found with counters I and II, the points obtained with counter III at the highest values of gas gain, in the region $\ln V > 8.1$, now fall below the extrapolation. In addition, the discharge mode of operation could not be observed with counter III. This behavior at very high values of $A$ implies that a distinctly different phenomenon has arisen in the multiplication process from that observed with counters I and II. The most obvious cause for this departure is the onset of saturation in the electron branching process due to space charge limitations in the neighborhood of the center wire. Once again, data obtained in this region cannot be truly representative of the electron multiplication process in proportional counters. However, below this region, the smooth monotonic behavior of $A$ implies that the corresponding single electron spectra should be representative of the electron branching process in proportional counters.

Some of the spectra observed in this region with counter III are displayed in Fig. 9. The low pulse-height extrapolation region, $\nu \leq (\nu_L/2)$, is depicted for each of these distributions. It is clear that the shape of the single electron distribution is not constant. At lower anode voltages the measured distribution decreases monotonically for all values of $\nu$, behaving approximately like an exponential distribution. As the anode voltage increases, a broad peak develops in the distribution. It must be emphasized that the nature of the change which arises in the single electron distribution cannot be readily attributed to saturation. One would expect that the strongest effect of saturation would be to weight the "tail" of these distributions more heavily. However, this does not occur. In view of this behavior, one can only conclude that the single electron distribution must depend upon gas amplification, i.e. $\bar{n}$.

The single electron distributions obtained with counter IV also support this conclusion. Table II reveals that counter IV, which may also be regarded as

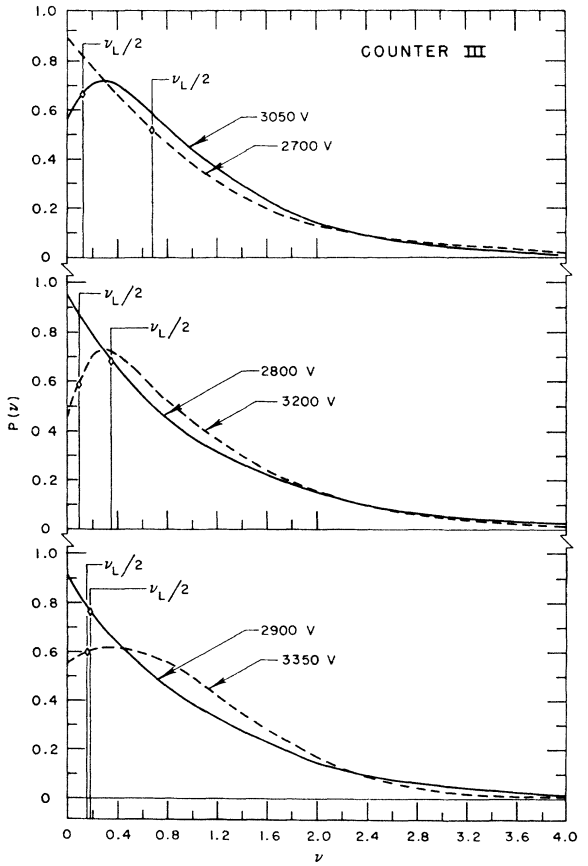


FIG. 9. The single-electron spectra obtained with counter III for anode voltages (a) 2700 and 3050 V. (b) 2800 and 3200 V. (c) 2900 and 3350 V.

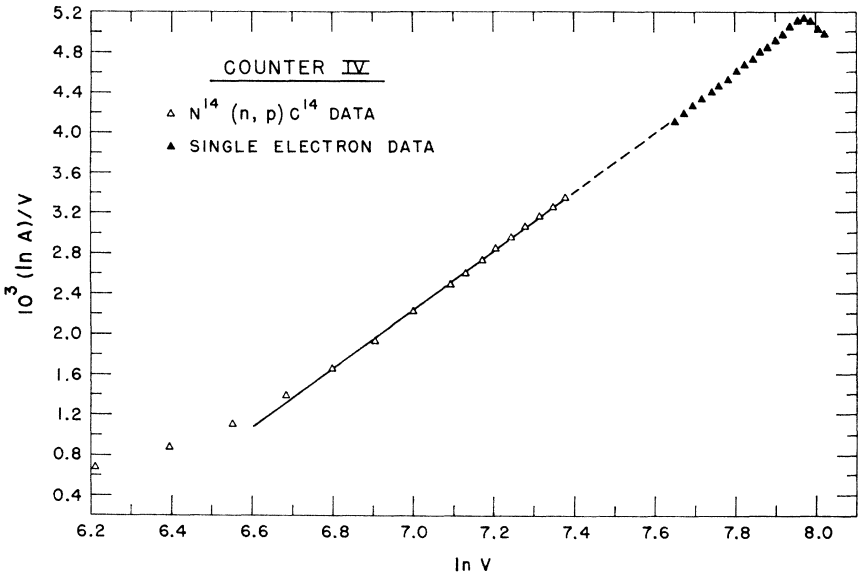


FIG. 10. The Diethorn representation of gas amplification $A$ as a function of anode voltage $V$ for counter IV.

a "pure" methane counter, contains half the absolute pressure utilized in counter III. The Diethorn representation of the gas gain data obtained with counter IV is given in Fig. 10. Here the onset of saturation in the region $\ln V > 7.95$ is also evident.

Comparison of Figs. 8 and 10 reveals that the gas gain behavior of counters III and IV are quite similar. For counter IV, as with counter III, one finds that $A$ increases at a slightly higher rate than predicted and a gradual deviation arises from the Diethorn representation in the single electron region. This departure implies that $[(\alpha/E)(V)]$ is not actually independent of $V$ over the entire range of experimental measurements. However, over a more restricted range of gas gain, this assumption is quite adequate. The data of counters III and IV indicate that the maximum range in gas gain over which the Diethorn representation is valid is the order of three decades.[17]

The single electron distributions obtained from counter IV have been compared with the results of counter III for the same value of $\bar{n}$. Such a comparison, which is presented in Fig. 11 for $\bar{n} \cong 1.25\times10^4$, $5.0\times10^4$, and $7.7\times10^4$, demonstrates that these distributions are similar for $\bar{n}$ less than approximately $10^5$. However, as $\bar{n}$ increases beyond $10^5$, the distributions obtained from these two counters begin to deviate. This is exhibited by the distributions obtained from $n \cong 2.7\times10^5$ and $3.8\times10^5$, which are displayed in Fig. 12.

The general nature of these proportional counter results are strikingly similar to the measurements of Schlumbohm,[15] who observed distributions from single electron avalanches in parallel plate chambers. The general status of parallel-plate observations is summarized in the monograph of Raether.[18] Since the parallel-plate configuration implies a constant field $E$, then $\alpha$ is a constant for these measurements. It is apparent that an analysis of the proportional counter configuration should utilize the extensive considerations which already exist for the simpler parallel plate configuration. Such a procedure is followed in the discussion of electron branching in proportional counters given below.

The relative variance, $\langle(\nu-1)^2\rangle_{av}$, of the single electron spectra obtained with counters III and IV is depicted in Fig. 13 as a function of $\ln\bar{n}$. As indicated earlier, the (higher) moments of the distribution are more sensitive to the extrapolation procedure than is the distribution $P(\nu)$ itself. The error bars given with each point in Fig. 13 are not the usual experimental error but represent a measure of the sensitivity of $\langle(\nu-1)^2\rangle_{av}$ to the extrapolation procedure. The relative variance has been obtained for these spectra using 10-, 15-, and 20-point least-squares extrapolation for the region $\nu \leq (\nu_L/2)$. The plotted points in Fig. 13 represent the average of these three values of $\langle(\nu-1)^2\rangle_{av}$ and the spread for each point is the absolute spread so obtained. Note the increase in sensitivity of the relative variance to the extrapolation procedure for the lower values of $\ln\bar{n}$. This behavior corresponds to the fact that $(\nu_L/2)$ increases with decreasing anode voltage.

The extrapolation of the relative variance to unity for low values of gas gain is supported by the actual behavior of $P(\nu)$ obtained at lower anode voltages. In this region, the single electron spectra decrease strictly monotonically and approximate a simple exponential distribution. The fact that the relative variance of an exponential distribution is unity and the observed spectra appear to approximate such a distribution at

[17] In this analysis, one must utilize large enough values of $A$ in order that the collection mode of operation can be neglected. To ensure that this condition is satisfied, one can utilize $A \gtrsim 10$ to define the proper lower bound of proportional counter operation.

[18] H. Raether, *Electron Avalanches and Breakdown in Gases* (Butterworths Scientific Publications, Inc., Washington, D. C., 1964).

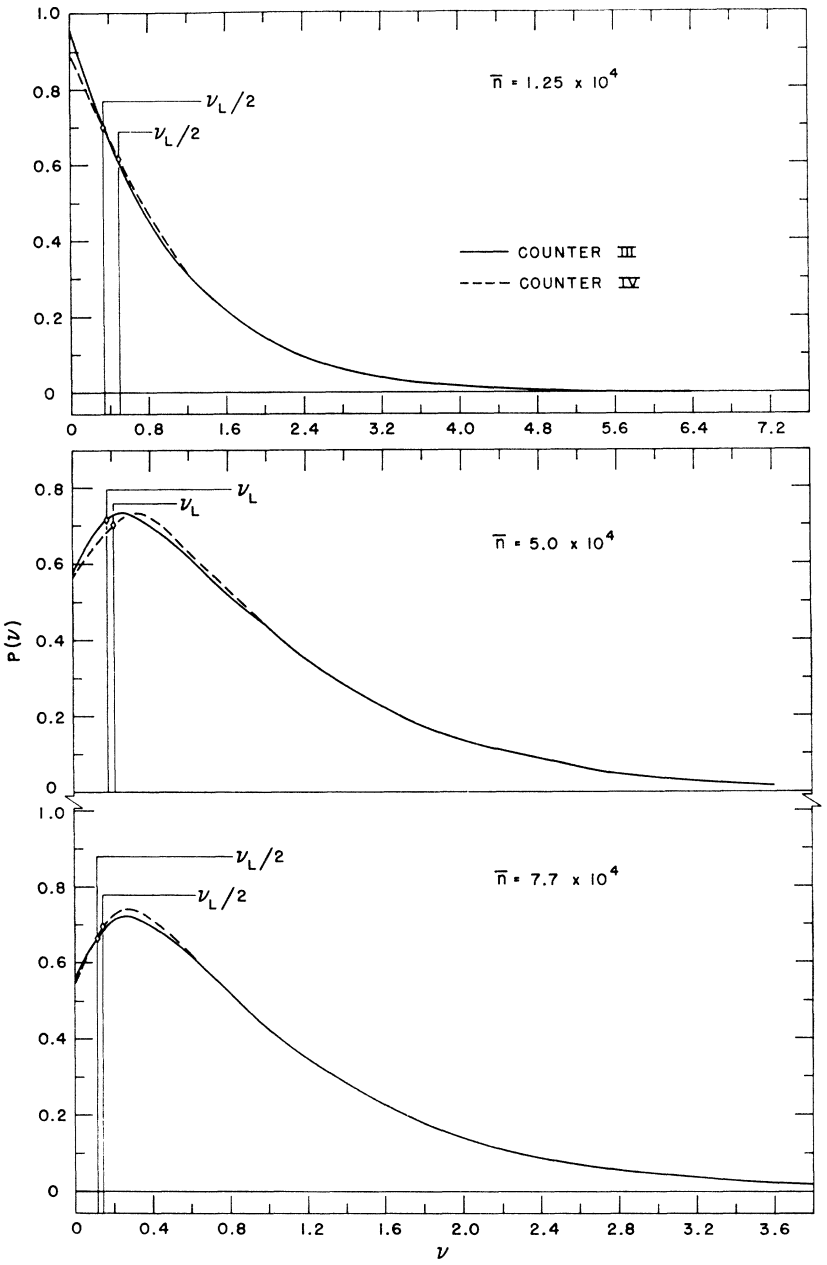


FIG. 11. Comparison of the single-electron spectra of counters III and IV for (a) $\bar{n}\cong 1.25\times 10^4$; (b) $\bar{n}\cong 5.0\times 10^4$; (c) $\bar{n}\cong 7.7\times 10^4$.

lower values of $\bar{n}$ support the suggested extrapolation of $\langle(\nu-1)^2\rangle_{av}$ in Fig. 13 to even lower values of $V$ or $\bar{n}$.

The relative variances displayed in Fig. 13 clearly demonstrate that the distributions obtained from counters III and IV coincide up to $\bar{n}\approx 10^5$ but begin to deviate beyond this point. It is important to note that the rapid increase in the relative variance of counter III, which arises for $\ln\bar{n}>13.0$, occurs simultaneously with the onset of saturation as demonstrated in Fig. 8 ($\ln V>8.1$). Consequently, the rapid change in the single electron spectrum of counter III, in the region $\ln\bar{n}>13.0$, can certainly be attributed to saturation effects. In fact, the effect of saturation in the counter III data undoubtedly extends below $\ln\bar{n}=13.0$ and probably influences the behavior of the relative variance in the region $12.0<\ln\bar{n}<13.0$. This follows from the fact that the relative variance (i.e., second moment) of the distribution $P(\nu)$ is obviously more sensitive to saturation phenomena than the mean value (i.e. first moment). Therefore, one must anticipate that the behavior of the relative variance will exhibit saturation somewhat earlier than the gas gain data.

The behavior of counter IV for $\bar{n}>10^5$ is clearly different from that of counter III. A monotonic increase in the relative variance begins at $\ln\bar{n}\cong 11.5$ which corresponds to $\ln V\cong 7.8$ in Fig. 10. At this point $A$ is

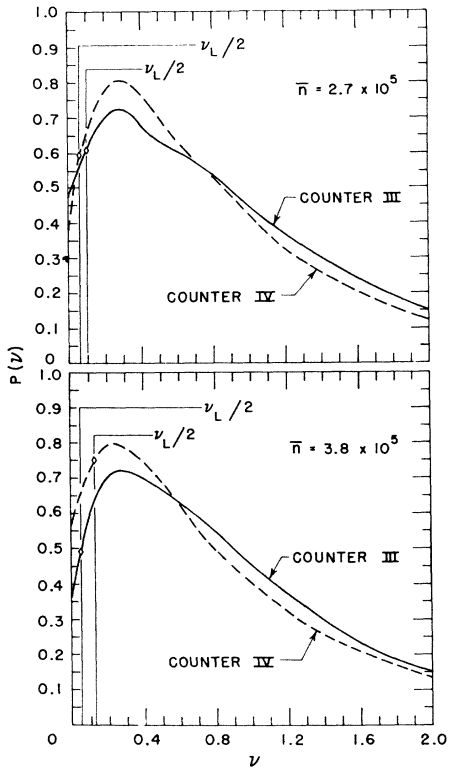


FIG. 12. Comparison of the single-electron spectra of counters III and IV for (a) $\bar{n}\cong 2.7\times 10^5$; (b) $\bar{n}\cong 3.8\times 10^5$.

still a smooth monotonically increasing function of $V$. Hence, the deviation of the distributions obtained from counters III and IV above $\bar{n}\cong 10^5$ can be attributed to the onset of saturation in counter III. On the other hand, the gradual increase of $\langle(\nu-1)^2\rangle_{av}$ for counter IV in the region $\bar{n}>10^5$ does not appear to be a result of saturation. This latter phenomenon must arise as an inherent aspect of the proportional counter multiplication process.

## IV. NON-MARKOVIAN MODELS

The fact that the single-electron spectrum is not constant but does depend upon $\bar{n}$ implies that the electron branching process is non-Markovian. The basic reason for this behavior has already been alluded to by Wilkinson,[19] West,[20] and Frisch.[4] Namely, that immediately after birth of an electron in the avalanche, it must travel some distance toward the wire before it acquires sufficient kinetic energy to produce further ionization. This model will be designated as the "delayed-Markovian" model. Legler[21] has analyzed this model and has applied it to the case of the parallel plate chamber. Moreover, the numerical results which have been obtained by Legler for the probability distribution $P(\nu)$ are in excellent agreement with the experimental measurements of Schlumbohm.[15,18]

On the other hand, the nonstationary Markovian model of Byrne[6] and Lansiart and Morucci[7] and the ordinary Markovian model[4,5] lead to a constant distribution for the multiplication process, which is not in agreement with the present experimental evidence. The general assumption of both Byrne and Lansiart and Morucci, that the multiplication process depends upon its past history is, in fact, only appropriate as an explanation for the observation of saturation. That is, once the electron branching process does become dependent upon its past history in this manner, one can anticipate the onset of such phenomena as saturation.

The general theory of non-Markovian stochastic branching processes has been introduced by Kendall[22] and Bellman and Harris.[23] The treatment of this subject, which is also called age-dependent stochastic branching theory, can also be found in general texts on branching theory.[24,25] This formulation of branching theory is expressed in terms of $F(s,t)$, the probability generating function corresponding to the desired probability distribution $P(\nu)$. Since this latter distribution is actually a function of the discrete variable $n$, it can also be denoted as $P_n$. Consequently, with $s$ as the dummy variable of the probability generation function $F(s,t)$, one can write

$$F(s,t)=\sum_{n=0}^{\infty} P_n(t)s^n, \tag{10}$$

where $F(s,t)$ satisfies the boundary data

$$F(s,0)=s. \tag{11}$$

Age-dependent branching theory yields a nonlinear integral equation for $F(s,x)$ of the form

$$F(s,t)=\int_0^t h[F(s,t-\tau)]g(\tau)d\tau+s[1-G(t)], \tag{12}$$

where

$$G(t)=\int_0^t g(\tau)d\tau \tag{13a}$$

and

$$h(s)=\sum_{n=0}^{\infty} q_n s^n. \tag{13b}$$

The branching process is characterized by the set of coefficients $\{q_n\}$ and the function $g(\tau)$. The set of coefficients $\{q_n\}$ of the function $h(s)$, which is also a probability generating function, are called transformation coefficients or transformation probabilities. The

[19] D. H. Wilkinson, *Ionization Chambers and Counters* (Cambridge University Press, London, 1950).
[20] D. West, Progr. Nucl. Phys. **III**, 18 (1953).
[21] W. Legler, Z. Naturforsch. **16a**, 254 (1961).
[22] D. G. Kendall, Biometrika **35**, 316 (1948).
[23] R. Bellman and T. Harris, Ann. Math. **55**, 280 (1952).
[24] A. T. Bharucha-Reid, *Elements of the Theory of Markov Processes and Their Applications* (McGraw-Hill Book Company, Inc., New York, 1960).
[25] T. E. Harris, *The Theory of Branching Processes* (Springer-Verlag, Berlin, 1963).

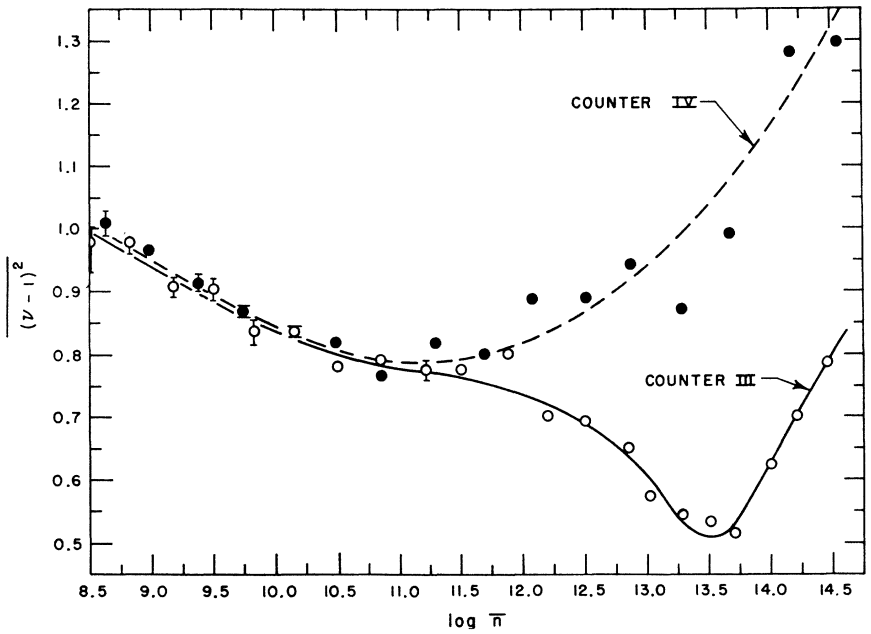


FIG. 13. The relative variance $\langle(\nu-1)^2\rangle_{av}$ as a function of $\ln\bar{n}$ for counters III and IV.

function $g(\tau)$ may be called the "birth generation" probability distribution. Here $g(\tau)d\tau$ represents the probability that an individual (electron) born at time $\tau=0$ be transformed at a time between $\tau$ and $\tau+d\tau$. For example, consider the case where the individual (electron) possesses a constant birth rate $\lambda$ for all $\tau$, $0\leq\tau<\infty$. In this event, the transformation of the individual is independent of $\tau$ (the Markov property) and one finds

$$g(\tau)=g_M(\tau)=\lambda e^{-\lambda\tau}. \tag{14}$$

Table III contains a list of the physical processes that can be associated with the simplest transformation coefficients. For the choice, $q_2\equiv 1$, $q_i\equiv 0$, $i\neq 2$, one has a binary branching model. Using this assumption, together with the birth generation probability distribution given in Eq. (14), the general age-dependent theory reduces precisely to a binary Markovian description. This result implies, in turn, that $P(\nu)$ will assume the simple exponential form.

From this viewpoint, the comments of Wilkinson,[19] West,[20] and Frisch,[4] mentioned above, are in reality qualitative statements concerning the behavior of $g(\tau)$ and the set of coefficients $\{q_n\}$ for electrons in a proportional counter. Recognition of the existence of a non-constant birth rate for electrons in the avalanche automatically implies that $g(\tau)$ and/or $\{q_n\}$ cannot be of the form assumed above and it follows that the branching process must be non-Markovian.

The experimental results presented above imply that binary Markovian branching is a good approximation at low values of gas gain. Hence any branching model introduced to explain electron multiplication in proportional counters must agree with this approach to Markovian behavior in the region of low gas gain.

Waugh[26] has introduced a general non-Markovian model which can be employed to satisfy this limiting condition. In the Waugh model, the transformation coefficients are functions of $\tau$, the age of the electron, i.e. $q_i=q_i(\tau)$, $i=1, 2\cdots$. Thus, if one chooses the Markovian birth-generation probability distribution $g(\tau)=g_M(\tau)$, then an approach to Markovian behavior will result if

$$\lim_{\tau\to 0} q_2(\tau)=1$$

$$\lim_{\tau\to 0} q_i(\tau)=0, \quad i\neq 2. \tag{15}$$

Unfortunately, the nonlinear integral equation which arises from the Waugh model is quite formidable, when one considers that even for the simplest binary branching models little or no success has been attained in finding analytical solutions of Eq. (12).[22–25] Numerical solutions of this equation are of little value since the desired probability distribution $\{P_n(t)\}$ is obtained from a series expansion of the analytical form of $F(s,t)$.

However, experimental results can be compared with different symmetrical binary branching models ($q_2\equiv 1$), since Bellman and Harris[23] have developed (asymptotic)

TABLE III. Physical properties of transformation coefficients.

| Transformation coefficient | Physical process |
|---|---|
| $q_0$ | Death (absorption) |
| $q_1$ | Scattering (elastic and inelastic) |
| $q_2$ | Birth (binary branching) |
| $q_3$ | Birth (ternary branching) |

[26] W. A. O'N. Waugh, Biometrika 45, 241 (1958).

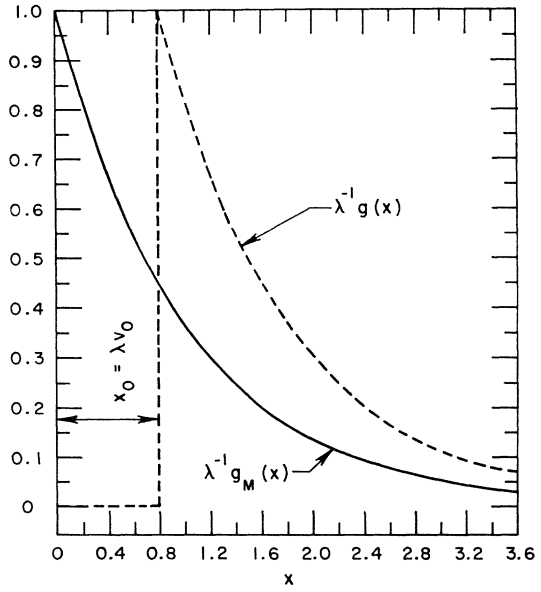


FIG. 14. A comparison of $g_M(x)$ with $g(x)$ of the "delayed-Markovian" model for $x_0=0.8$.

formulas for the moments of the desired probability distribution. In particular, it is of interest to examine the "delayed-Markovian" model which has proven so successful for the parallel plate configuration.

In terms of the present application, the variable $\tau$ actually represents the potential difference $v$, traversed by the electron from birth. Introducing this change in notation, the birth generation function for the "delayed-Markovian" model is given by:

$$\begin{aligned} g(v)&=0, && v<v_0,\\ g(v)&=\lambda e^{-\lambda(v-v_0)}, && v\geq v_0. \end{aligned} \tag{16}$$

Here $v_0$ represents the ionization potential of the gas and $\lambda^{-1}$ is the average potential difference traversed between ionizing collisions. In terms of the variable $x=\lambda v$, this birth generation probability distribution takes the form

$$\begin{aligned} g(x)&=0, && x<x_0,\\ g(x)&=\lambda e^{-(x-x_0)}, && x\geq x_0, \end{aligned} \tag{17}$$

where $x_0=\lambda v_0$. Figure 14 presents a comparison between this choice of $g(x)$, for $x_0=0.8$, and $g_M(x)$.

A second birth generation probability distribution function will also be considered. It is a special case of the original form of $g(\tau)$ studied by Kendall.[22] For the Kendall model, we have chosen

$$g(v)=\frac{(1+\rho)^{1+\rho}}{\Gamma(1+\rho)}\lambda^{1+\rho}e^{-\lambda(1+\rho)v}v^{\rho}, \tag{18}$$

where $\Gamma$ is the customary notation for the gamma function. In terms of $x=\lambda v$, one has

$$g(x)=\frac{(1+\rho)^{1+\rho}}{\Gamma(1+\rho)}\lambda e^{-(1+\rho)x}x^{\rho}. \tag{19}$$

In this model $g(x)$ rises from zero, passes through a peak and then monotonically decreases to zero. The parameter $\rho$ and the position of the peak at $v=v_0'$ (or $x=x_0'$) are related by the condition

$$\rho=\frac{\lambda v_0'}{1-\lambda v_0'}=\frac{x_0'}{1-x_0'}. \tag{20}$$

This choice of $g(x)$, for $\rho=\frac{1}{2}$ ($x_0'=0.33$), is depicted in Fig. 15 in comparison with $g_M(x)$. The parameters $\lambda$ and $v_0'$ play an identical role in the "Kendall" model to the parameters $\lambda$ and $v_0$ of the "delayed-Markovian" model.

Figure 16 presents the (asymptotic) relative variances calculated from the Bellman-Harris theory for these two models. Note that for $x_0\to 0$ and $x_0'\to 0$ that these two models approach Markovian behavior. This fact also follows directly from Eqs. (17) and (19), since $g(x)\to g_M(x)$ for $x_0\to 0$ and $x_0'\to 0$, respectively. Hence, both the "delayed-Markovian" and "Kendall" models will satisfy the necessary limiting condition of Markovian behavior at low gas gain provided $x_0$ and $x_0'$ become small for low gas gain. However, for these two models, $\lambda=\alpha(E)/E$ is assumed constant, which implies $x_0$ and $x_0'$ are also constant. Since this is not the case for proportional counters (viz. Fig. 3), these models can at most be viewed as rough approximations even when representative or average values of $\lambda$ are chosen. Consequently, these models will only be employed to furnish a qualitative understanding of the proprotional-counter multiplication process.

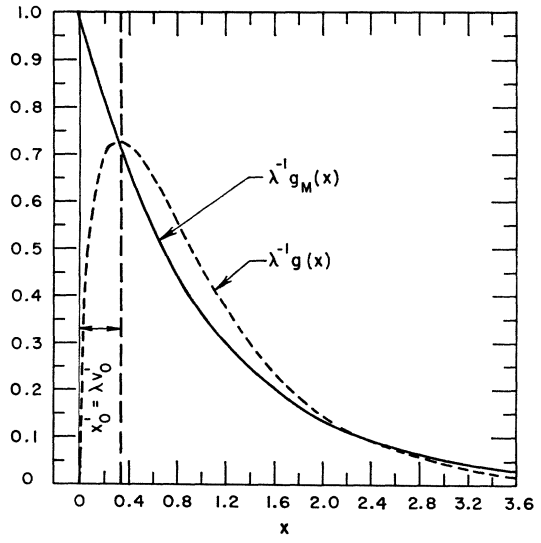


FIG. 15. A comparison of $g_M(x)$ with $g(x)$ of the "Kendall" model for $x_0'=0.33$.

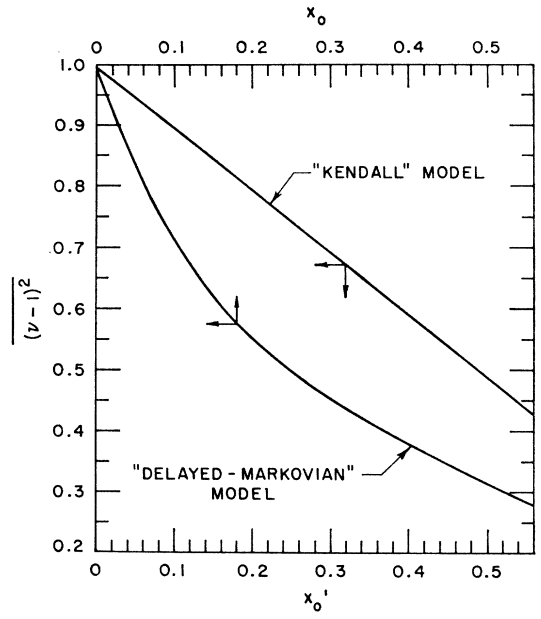


FIG. 16. A comparison of the asymptotic relative variances of the "delayed-Markovian" and "Kendall" models as functions of $x_0$ and $x_0'$, respectively.

In contrast with the behavior of gas gain (i.e. $\bar{n}$), which could be adequately described by assuming that $\lambda=[(\alpha/E)(V)]$ is constant, it is apparent that the fluctuations which arise in the multiplication process must depend on the detailed behavior of $\lambda=[\alpha(E)/E]$. Moreover, it is also clear that the critical radius $r_c$ or the corresponding critical field-to-pressure ratio, which are also introduced in the description of gas gain, are actually average or representative values. Indeed, the very fluctuations inherent in these variables underlie the behavior of $P(\nu)$.

In particular, the behavior of $\lambda=\alpha(E)/E$ at the very early stages of the multiplication process is crucial. Thus if $\lambda=\alpha(E)/E$ is small (hence, $x_0$ and $x_0'$ are small) in the early stages and the total multiplication is not too large, then the process can possess a "memory" and will reflect the Markovian behavior of the earlier stages. However, for increasing anode voltage the value of $\lambda=\alpha(E)/E$ will increase even for the early stages of the multiplication process. Furthermore, the increase in gas gain will tend to divorce the end result from the early stage fluctuations and thus the process will tend to lose "memory" of its origin. Consequently, the multiplication process will exhibit continuous deviation from Markovian behavior.

However, as the anode voltage is increased even farther, one can anticipate that the plateau which arises in $[\alpha(E)/E]$ will be reflected in the behavior of the distribution, $P(\nu)$. Indeed, the relative variance data of Fig. 13 shows that a slowly varying behavior does arise in the region $10.5\leq\ln\bar{n}\leq12.0$. For $\ln\bar{n}\geq12.0$, the counter III data is influenced by saturation and the counter IV data may reflect the fact that $\alpha(E)/E$ begins to decrease for this domain of proportional counter operation. Hence, only in this region will it be meaningful to make comparisons between experimental results and the simplified binary branching models introduced above.

Corresponding to the region $10.5\leq\ln\bar{n}\leq12.0$, two representative values for both $x_0$ and $x_0'$ can be obtained. Using the $[E/\alpha(E)]$ data given in Fig. 3 for methane, one finds a plateau value of $\lambda^{-1}\cong65$ V. The Diethorn representations of gas gain given in Figs. 8 and 10 for counters III and IV yield $\lambda^{-1}\cong[(\alpha/E)(V)]\cong44$ V. Since $v_0=13.3$ V for methane, these two estimates of $\lambda$ indicate that both $x_0$ and $x_0'$ lie in the region 0.20–0.30. Here the corresponding relative variance predicted by the "delayed-Markovian" model ranges from 0.55–0.45, while the corresponding relative variance of the "Kendall" model varies from 0.80–0.70. Figure 13 reveals that the experimental value of $\langle(\nu-1)^2\rangle_{\text{av}}$, in the region $10.5\leq\ln n\leq12.0$, lies close to 0.80. Thus the "Kendall" model would appear to have greater validity for this region of proportional-counter operation.

On the basis of this qualitative discussion, it is clear that these simple non-Markovian binary branching models are not generally adequate. A more general treatment is necessary in order to describe the entire scope of the proportional counter multiplication process properly. Only the more complex branching models, such as the Waugh model, which has been briefly described above, afford such a possibility.

## ACKNOWLEDGMENT

The authors gratefully acknowledge the assistance of Miss Ingeborg Olson who wrote the computer program utilized in the analysis of the experimental data.